

## The Possible Ameliorative Effect of Selenium and Vitamins Combination against Amiodarone-Induced Alveolar Damage in Albino Rat: Histological and Immunohistochemical Study

Amal A. Mahdy

Anatomy and Embryology Department, Faculty of Medicine, Tanta University, Gharbia, Egypt  
[mora2004@live.com](mailto:mora2004@live.com)

**Abstract: Background:** Chronic interstitial pneumonitis is the most common presentation of amiodarone-induced pulmonary disease. **Aim of the work:** To throw a light on the damage of the rat lung following amiodarone administration and to evaluate whether selenium and vitamins combination ameliorate this effect on the rat lung alveoli. **Material and methods:** Twenty adult male albino rats were divided into three groups. The first was control group. The second group received amiodarone (30 mg/Kg/day) for six weeks. The third group received amiodarone as well as selenium and vitamins combination for six weeks. Fibrosis fraction, alveolar wall area fraction in addition to PCNA labeling index of the lung alveoli were measured by using image analyzer and the measured data were statistically analyzed. **Results:** After amiodarone administration, the lung showed injured as well as collapsed alveoli, mononuclear cell infiltration, thickening of the wall of the bronchioles and pulmonary arterioles with obstruction of some bronchioles. Significant increase in the area % of the inter-alveolar collagen and area % of the alveolar wall was detected. Also, significant increase in the PCNA labeling index of the alveolar cells was noted. By SEM, increased thickness of the inter-alveolar septa and laceration of the alveolar lining cells which were mostly formed of type II pneumocytes were observed. All findings regressed after selenium and vitamins administration. **Conclusion:** This study has important implications for the treatment of amiodarone-induced lung damage and fibrosis.

[Amal A. Mahdy. **The Possible Ameliorative Effect of Selenium and Vitamins Combination against Amiodarone-Induced Alveolar Damage in Albino Rat: Histological and Immunohistochemical Study.** *J Am Sci* 2014;10(4s):61-71]. (ISSN: 1545-1003). <http://www.jofamericanscience.org>. 8

**Keywords:** Amiodarone, lung, image analyzer, selenium, vitamins, histological, PCNA.

### 1. Introduction

Amiodarone is an iodinated benzofuran derivative that is highly effective in suppressing ventricular and supraventricular tachyarrhythmias. Pulmonary toxicity as chronic interstitial pneumonia, organising pneumonia, diffuse alveolar damage and even acute respiratory distress syndrome are common and can predispose to lung fibrosis (Naidich *et al.*, 2007). Also, amiodarone can cause a variety of adverse side effects including photosensitivity, blue-gray discoloration of the skin, thyroid dysfunction, corneal deposits, abnormal liver function tests, and bone marrow suppression (Larsen *et al.*, 2012).

The mechanisms of amiodarone pulmonary injury include direct toxicity to lung tissue, hypersensitivity reaction to amiodarone, and enhanced oxidative stress. Alteration of membrane properties and activation of alveolar macrophages and cytokine release are the other proposed mechanisms of amiodarone toxicity (Bolt *et al.*, 2001; Punithavathi *et al.*, 2003).

Pulmonary fibrosis is a progressive and essentially untreatable disease with a fatal outcome. Typical features in this disease include dyspnea, diffuse interstitial infiltrates and poor prognosis. There are five million people worldwide that are affected by this disease. No effective treatment was

confirmed for pulmonary fibrosis except lung transplantation (O'Brien *et al.*, 2011). The pathogenesis of pulmonary fibrosis remains incompletely understood, but lung inflammation is a major underlying component of a wide variety of pulmonary fibro-proliferative disorders (Zhang & Phan, 1996; Cocker & Laurent, 1997; Hemmati *et al.*, 2006).

Vitamin E alone was used as an antioxidant to relieve the lung injury produced by amiodarone but the protection was incomplete (Zidan, 2011). Antioxidant vitamins C, E,  $\beta$ -caroten and selenium have been studied for their capacity to protect human cells from damage induced by radiation (Konopacka & Rzeszowska-Wolny, 2001). Additive and synergistic interactions occur among antioxidants. This synergism strengthens the protection provided by an individual antioxidant alone (Chen & Tappel, 1995). In the current study we investigated the lung damage induced by amiodarone and the possible preventive role of selenium in addition to combined vitamins against the amiodarone-induced alveolar fibrosis and damage in adult male albino rats.

### 2. Material and Methods

**Animals:** Twenty adult Sprague Dawley male rats weighing 150-200 gm at the start of the

experiment were used. They were kept under good hygienic conditions, fed *ad libitum* and allowed for free water supply in Anatomy Department, Animal House, Faculty of Medicine, Tanta University. The animals were acclimated to these conditions at least 1 week before receiving the treatment. The rats were treated in accordance with guidelines approved by the Animal Use Committee of Tanta University.

**Drug:** Amiodarone was given in the form of tablet (Cordarone<sup>®</sup>, 200 mg) that was donated from Global Napi Pharmaceuticals, Egypt. The desired daily dose (30 mg/kg body weight) was dissolved in 3 ml of 0.6% methylcellulose (Kolettis *et al.*, 2007) and orally administrated by orogastric tube (Zaglool *et al.*, 2011). Methylcellulose was obtained from El-Gomhoria, company for chemical and medical trading, Tanta, Egypt.

Selenium-ACE tablets were used as antioxidants against the damage produced by amiodarone. It was obtained from Interpharma Company. Each tablet contains: Vit A (1.500 IU), Vit C (90mg), Vit E (30mg) and Selenium (100µg). The recommended human daily dose is one tablet/day. Each tablet was dissolved in 25ml distilled water and was orally administrated once daily as 0.5ml/rat by orogastric tube (Refaat, 2007).

**Experimental procedure:** The rats were divided into three groups, ten rats for group I (control) and five rats for each of group II as well as group III. Rats of group I were divided into two equal subgroups. Subgroup Ia did not exposed to any procedure and were considered negative control group. The subgroup Ib received 3 ml of 0.6% methylcellulose (vehicle of amiodarone) through an orogastric tube daily for 6 weeks. The rats of group II were given the daily dose of amiodarone orally 6 days/ week for 6 weeks (Zaglool *et al.*, 2011). The rats of group III received the daily dose of amiodarone (30mg/kg/day) and the Selenium-ACE tablets for 6 weeks orally 6 days/ week for 6 weeks. At the end of the experiment, animals were anesthetized with ether inhalation. The chest was opened and specimens of the left lung were fixed in 10% formalin, dehydrated through an ethanol series, cleared and embedded in paraffin. Five micrometer sections were stained with hematoxylin and eosin for histopathological evaluation as well as Mallory's trichrome for demonstration of collagen fibers (Bancroft & Gamble, 2008). Additional sections were immunostained to examine the proliferating cell nuclear antigen (PCNA) in the alveolar wall. The PCNA is an endogenous nuclear protein that is used as a suitable marker for cell proliferation and is synthesized in late G1 and S phases of the cell cycle (Foley *et al.*, 1991). The right lung specimens were

processed for scanning electron microscopic examinations.

**Immunohistochemical study:** The sections were deparaffinized in xylene and hydrated in decreasing concentrations of ethanol. Endogenous peroxidase was blocked by incubation in 3% hydrogen peroxidase for 30 minutes. The sections were then washed with phosphate-buffered saline (PBS) and incubated overnight in a humid chamber at 4°C with monoclonal anti-PCNA antigen (PC10-antibody). Sections were washed three times with PBS, incubated for 1 hour with peroxidase-labelled IgG followed by diaminobenzidine for staining the PCNA-bound complex. The sections were counterstained with Harris hematoxylin, dehydrated and mounted (Korkolopoulou *et al.*, 1993).

**Scanning electron microscopic examination:** The specimens of right lung were immersed in 2.5% glutaraldehyde, washed five times with 0.1 M phosphate buffer solution and emerged for 12 hours. The specimens were placed in a solution formed of osmium tetroxide in 1% phosphate buffer solution 0.1 M for 1 hour at 4°C. Following that, lung specimens were washed in 3 baths of bi-distilled water for 2 to 3 minutes each and immersed in aqueous tannic acid solution at 1 % per hour at 4°C. After that the specimens were dehydrated with ethanol in crescent concentrations of 50%, 70%, 90% and 95% for 10 minutes each. Then the samples were dried in SPI supplies, critical point drying machine using liquid CO<sub>2</sub>. The samples were mounted on aluminum stubs, coated by gold in a SPI-Module<sup>TM</sup> Vac / sputter (Bozzola & Russel, 1999). Then the specimens were photographed using JEOL, JSM-52500 LV scanning electron microscope, Japan at Faculty of Medicine, Tanta University, Tanta, Egypt.

**Morphometric study:** By using "Leica Qwin DFC 290 HD" software image analyzer computer system, the following measurements in control and experimental groups were done then the measured data were recorded and statistically analyzed.

(a) Fibrosis fraction. The degree of fibrosis was quantified by analyzing slides that were stained with a Mallory's trichrome stain. The image analysis program was configured to detect areas of blue-stained collagen within each field. At a magnification of 400, ten randomly selected constant fields per slide were selected. The fraction of blue-stained collagen areas for each field was averaged for each animal. The area fraction of fibrosis is presented as a percentage (Izbicki *et al.*, 2002).

(b) Alveolar wall area fraction was performed in H & E stained sections at a magnification of 100. Ten randomly selected fields lacking visible blood vessels and airways were selected using the video camera and displayed on the monitor. The image

analysis software was programmed to measure the area of all alveolar wall stained tissue and divide it by the constant field of interest area, thereby calculating an alveolar wall area fraction value for 10 fields. Data are presented as a percentage (Izbicki *et al.*, 2002).

(c) The PCNA Labeling Index (PCNA- LI) of the alveolar cells in PCNA immunostained section was determined by dividing the number of PCNA stained cells (had brown colored nuclei of all intensity) in ten non overlapping fields for each animal by the total number of evaluated cells at a magnification of 400 then multiplying by 100 (Korkolopoulou *et al.*, 1993). The other positive cells were not considered in this study.

*Statistical analysis:* The results are expressed as the mean  $\pm$  SD. Paired t tests was used for statistical comparisons. All statistical analyses were performed using Statistical Package for Social Sciences software (SPSS), Version 13.0 for Microsoft Windows. *P* value  $<$  0.05 was considered statistically significant whereas *p* value  $<$  0.01 was considered statistically highly significant (Dawson-Saunders & Trapp, 2001).

### 3. Results:

#### Light microscopic results:

##### Group I:

Examination of sections of control rats revealed that the lung was composed of numbers of bronchioles. Each of them were surrounded by smooth muscle layer and accompanied by a pulmonary arteriole and venuole. Alveolar ducts containing openings of many alveoli in their wall were seen. Large number of alveolar sacs in which some alveoli opened could be observed (Fig. 1). The alveoli were separated by thin inter-alveolar septa which had rich plexuses of capillaries. The wall of each alveolus was formed of different types of cells including macrophages which were present also in their cavities. The lining epithelium of the alveoli (alveolar cells) was formed mainly of squamous type I pneumocytes having flat nuclei and cuboidal type II pneumocytes (Figs. 2, 3). Mallory's trichrome stained sections showed normal collagen fiber distribution in the alveolar walls as well as around the blood vessels and bronchioles (Fig. 4). The PCNA positive cells were hardly detected in the alveolar cells (Fig. 5).

##### Group II:

The lung of group II showed thickened smooth muscle layer of the bronchioles. Some of small bronchioles showed obliteration of their lumens by epithelial cells. Also, the pulmonary arterioles were congested and had thick wall. Collapse of the alveoli with mononuclear cell infiltration around the

blood vessels could be demonstrated. Presence of hemorrhage, hyaline material and cellular debris in the lumen of few alveoli were detected (Figs. 6, 7). The alveolar wall was formed mainly of type II pneumocytes. Thickening of the inter-alveolar septum and presence of large number of macrophage as well as fibroblasts in the lumen of the alveoli could be noted (Fig. 8). Extensive fibrosis with increase in the collagen deposition around the alveoli as well as around the blood vessels and the bronchioles was observed (Fig. 9). Increased number of PCNA positive nuclei in the alveolar cells was noted (Fig. 10).

##### Group III:

The rat lung of group III showed apparently normal thickness of the pulmonary arteriole wall and of the bronchioles smooth muscle layer. Normal sized air spaces as alveolar sacs and alveoli with thin inter-alveolar septa could be seen (Fig. 11). They were lined by type I and type II pneumocytes in addition to macrophages (Fig. 12). Normal collagen deposition around the alveoli as well as around the blood vessels and the bronchioles was detected (Fig. 13). Mild increase in the number of PCNA positive nuclei of alveolar cells was noted as compared to the control group (Fig. 14).

#### Scanning electron microscopic results:

##### Group I:

The specimens of control rat lung showed small bronchiole surrounded by a smooth muscle layer and accompanied by pulmonary arteriole. Air spaces with alveoli openings into their wall and numerous alveoli were observed. The neighboring alveoli were separated by thin inter-alveolar septa (Fig. 15). The alveoli were lined by squamous type I pneumocytes and cuboidal type II pneumocytes while the luminal surfaces of the bronchioles revealed apical surfaces of Clara cells with number of ciliated cells in between (Figs. 16, 17).

##### Group II:

The rat lung specimens of group II showed increased smooth muscle layer thickness of the bronchioles and presence of collapsed alveoli as well as narrow openings of the alveoli in the wall of air spaces. Increased thickness of the inter-alveolar septa was noted (Figs. 18, 19). The lining epithelium of the alveoli was mainly formed of type II pneumocytes with some areas revealing cell laceration. The luminal surface of the bronchioles exhibited loss of cilia in between the Clara cells with disorganization and atrophy of cilia in some areas (Figs. 20, 21).

**Group III:**

The examination of rat lung specimens of group III showed apparent normal thickness of the bronchiole's smooth muscle layer and normal sized alveoli. The openings of the alveoli into the air spaces as well as the inter-alveolar septa thickness were apparently normal sized (Fig. 22). The lining epithelium of the alveoli were formed of type I pneumocytes and type II pneumocytes. It revealed damage of cells in small areas (Fig. 23). The luminal surface of the bronchioles exhibited normally appeared apical surface of Clara cells. Loss of cilia was observed but in lesser extension as compared to group II (Fig. 24).

**Quantitative results:**

The collagen fiber area percentages of group II rats revealed highly significant increase in comparison with that of the control rats. On the other hand, the collagen fiber area percentages of group III rats were within the normal values with highly significant decrease as compared to that of group II. Estimation of the alveolar wall area percentages of group II rats showed also significant increase as compared to that of the control rats. In group III rats, the alveolar wall area percentages exhibited insignificant differences. Proliferation of the alveolar cells, as indicated by PCNA labeled index, revealed highly significant increase in group II rats comparing with that of the control rats. As regards the PCNA labeled index of the alveolar cells of group III rats, highly significant decrease was recorded in comparison with that of group II. Regarding the control rats, a highly significant increase in the PCNA labeled index was recorded (Table. 1).

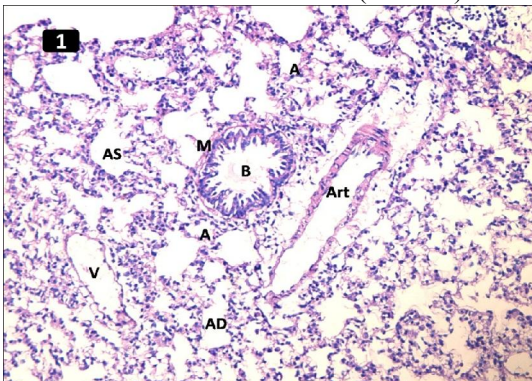


**Fig. 1:** A photomicrograph of a section in rat lung of the control group showing a bronchiole (B) surrounded by smooth muscle layer (M). Pulmonary arteriole (Art) and venule (V) are noted. Air spaces as alveolar ducts (AD), alveolar sac (AS) and alveoli (A) can be seen. H&E, X 200.

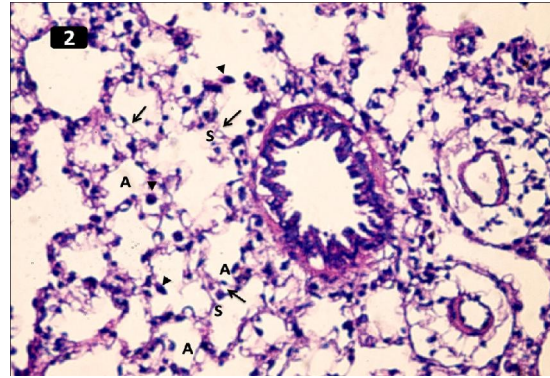


**Fig. 2:** A photomicrograph of a section in rat lung of the control group showing numerous numbers of alveoli (A). The wall of each alveolus is formed of different types of cells. The alveoli are separated by thin inter-alveolar septa (S) containing plexus of capillaries (↑). Some of the alveoli contain macrophages (▲) in their cavities. H&E, X 400.

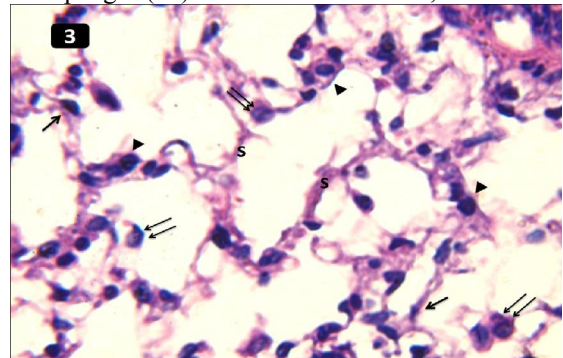


**Fig. 3:** A magnified photomicrograph of a section in rat lung of the control group showing the squamous type I pneumocytes (↑) and cuboidal type II pneumocytes (▲) forming the lining epithelium of the alveoli. Large number of macrophage (↑↑) is seen inside or in the wall of the alveoli. Thin inter-alveolar septa (S) can be noted. H&E, X 1000.

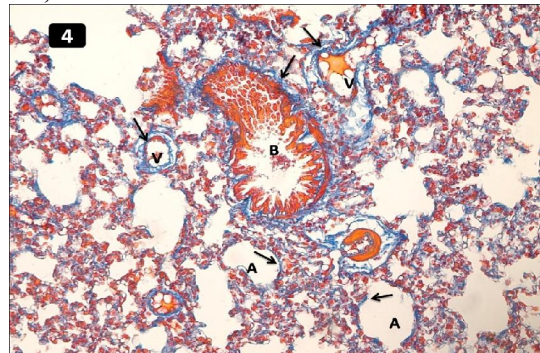


**Fig. 4:** A photomicrograph of a section in rat lung of the control group showing normal collagen distribution (↑) in the alveolar walls around the alveoli (A) as well as around the blood vessels (V) and bronchioles (B). Mallory's trichrome, X 200.

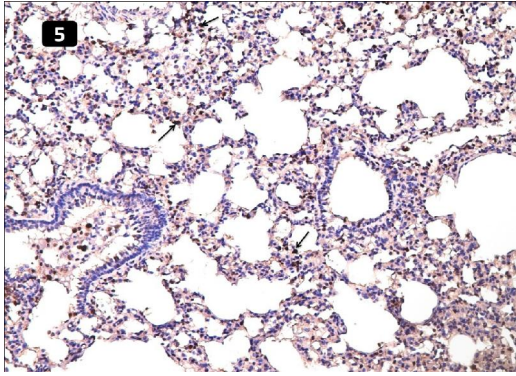


**Fig. 5:** A photomicrograph of a section in rat lung of the control group showing PCNA positive nuclei (↑) of the alveolar cells. Immunostaining for PCNA, X 200.

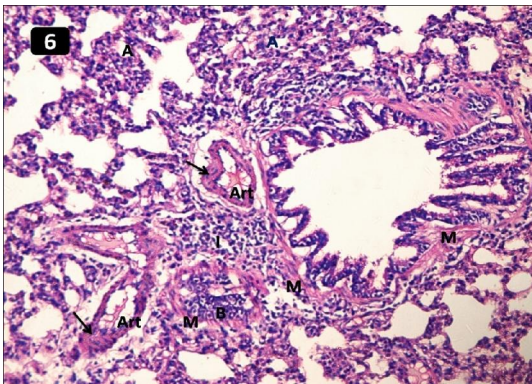


**Fig. 6:** A photomicrograph of a section in rat lung of the group II showing bronchioles having thick smooth muscle layer (M). Some of them (B) are obliterated by epithelial lining cells. Also, the pulmonary arterioles (Art) are congested and have thick wall. Collapse of the alveoli (A) and perivascular mononuclear cell infiltration (I) can be demonstrated. H&E, X 200.

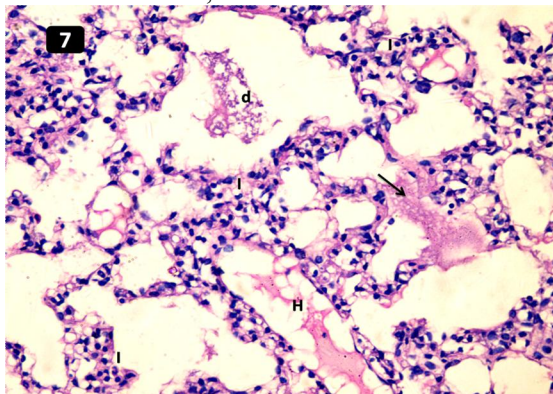


**Fig. 7:** A photomicrograph of a section in rat lung of the group II showing presence of hyaline material (↑), intra-alveolar hemorrhage (H) and cellular debris (d) in the lumen of few alveolar spaces. Mononuclear cell infiltration (I) can be seen in the alveolar walls. H&E, X 400.

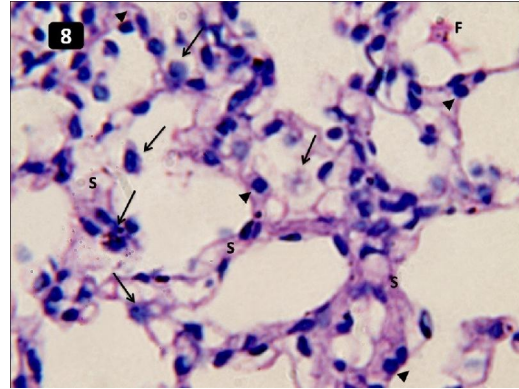


**Fig. 8:** Magnified photomicrograph of a section in rat lung of the group II showing thickened intra-alveolar septum (S). The alveolar wall is formed mainly of type II pneumocytes (▲). Large number of macrophage (↑) and presence of fibroblasts (F) in the lumen of the alveoli can be noted. H&E, X 1000.

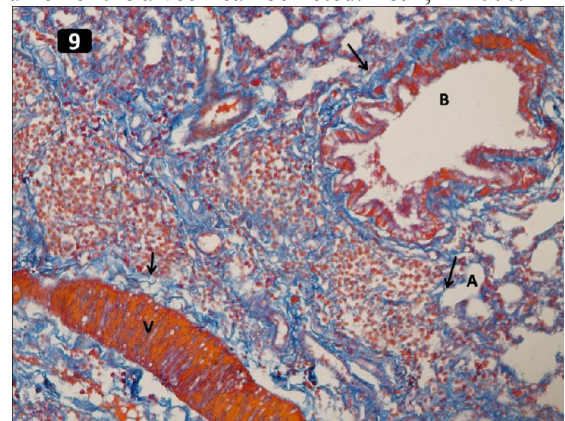


**Fig. 9:** A photomicrograph of a section in rat lung of the group II showing extensive fibrosis with increase in the collagen deposition (↑) around the alveoli (A) as well as around the blood vessels (V) and the bronchioles (B). Mallory's trichrome, X 200.

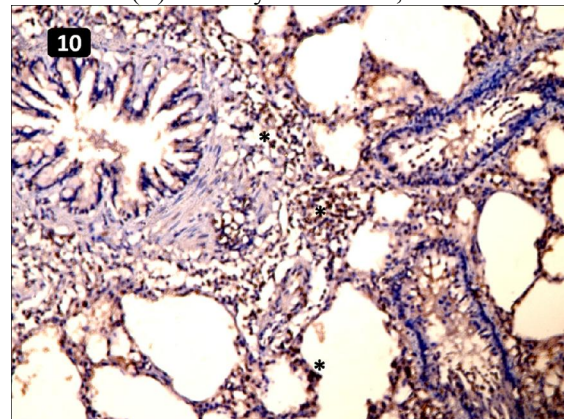


**Fig. 10:** A photomicrograph of a section in the rat lung of the group II showing increase in the PCNA positive nuclei number of the alveolar cells (\*). Immunostaining for PCNA, X 200.

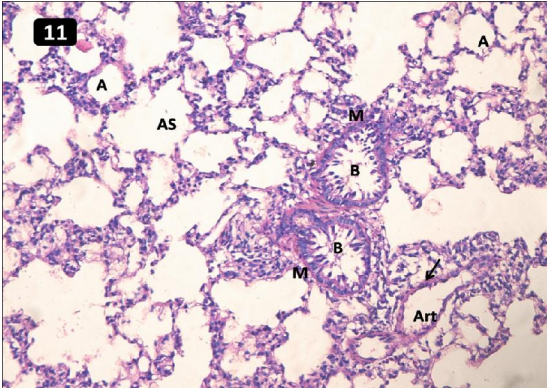


**Fig. 11:** A photomicrograph of a section in rat lung of the group III showing bronchioles (B) with normal smooth muscle layer (M) thickness. The wall of pulmonary arteriole (Art) has apparent average thickness (↑). Normal sized air spaces as alveolar sac (AS) and alveoli (A) can be seen. H&E, X 200.

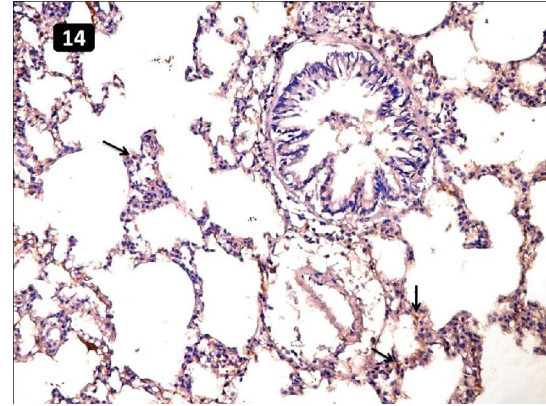


**Fig. 14:** A photomicrograph of a section in rat lung of the group III showing mild increase in the PCNA positive nuclei number in the alveolar cells (\*). Immunostaining for PCNA, X 200.

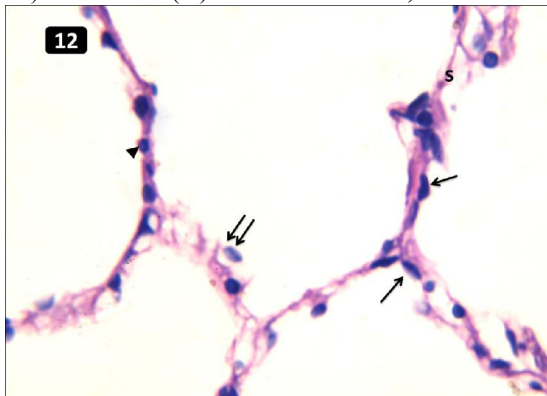


**Fig. 12:** A magnified photomicrograph of a section in rat lung of the group III showing normally appeared alveoli with type I pneumocytes (↑) and type II pneumocytes (▲) in their wall. Presence of macrophages (↑↑) and thin inter-alveolar septa (S) are also seen. H&E, X 1000.

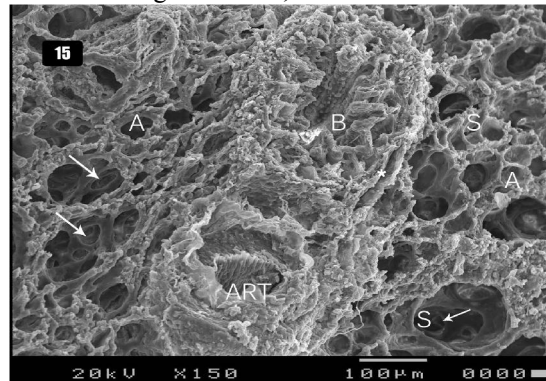


**Fig. 15:** A scanning electron photomicrograph of a section in rat lung of the control group showing small bronchiole (B) with normal smooth muscle layer thickness (\*) and pulmonary arteriole (ART) close to it. Alveoli openings (↑) which open into the alveolar duct wall are observed. Numerous normal sized alveoli (A) having thin inter-alveolar septa (S) between them are seen. Mic. Mag. X 150.

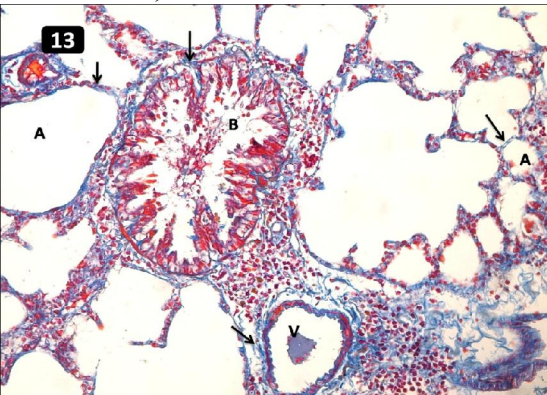


**Fig. 13:** A photomicrograph of a section in rat lung of the group III showing normal distribution of collagen fiber (↑) around the alveoli (A) as well as around the blood vessels (V) and the bronchioles (B). Mallory's trichrome, X 200.

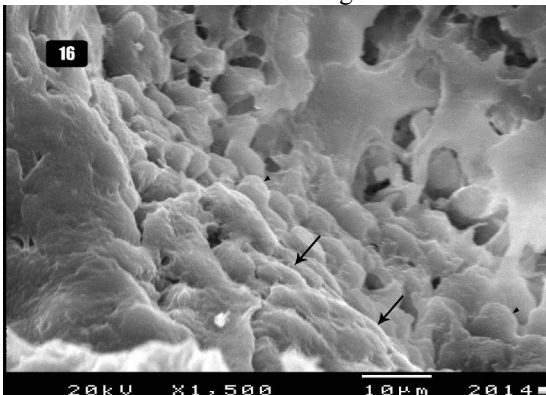


**Fig. 16:** A scanning electron photomicrograph of a section in rat lung of the control group showing squamous type I pneumocytes (↑) and cuboidal type II pneumocytes (▲) in the wall of the alveoli. Mic. Mag. X 1500.

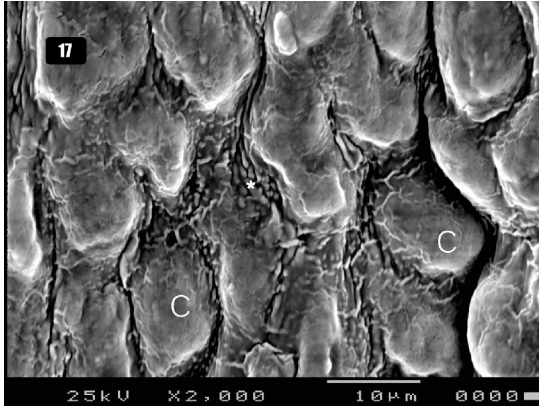


**Fig. 17:** A scanning electron photomicrograph of a section in the luminal surface of control rat bronchiole showing apical surface of the lining Clara cells (C) with few ciliated cells lying in between them (\*). Mic. Mag. X 2000.

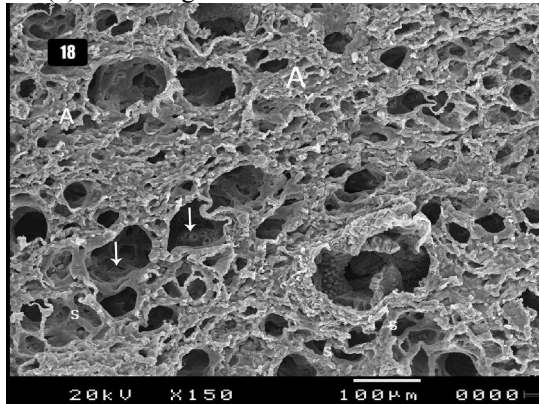


**Fig. 18:** A scanning electron photomicrograph of a section in the rat lung of group II showing collapsed alveoli (A) in most of the fields with alveolar ducts (AD) having narrow alveoli openings into its wall (↑). Increased thickness of the inter-alveolar septa (S) between the alveoli can be observed. Mic. Mag. X 150.

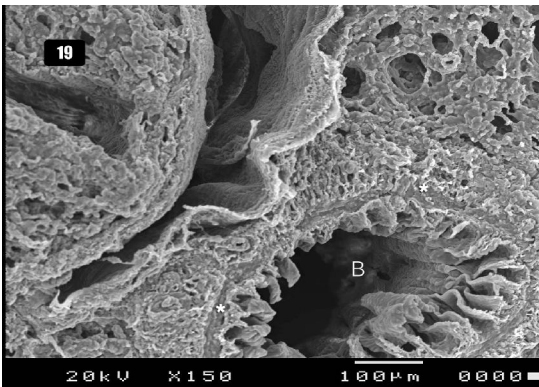


**Fig. 19:** A scanning electron photomicrograph of a section in the rat lung of group II showing increased smooth muscle layer thickness (\*) of a small bronchiole (B). Mic. Mag. X 150.

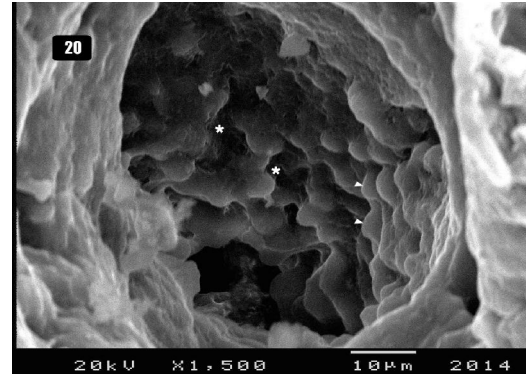


**Fig. 20:** A scanning electron photomicrograph of a section in the rat lung of group II showing that the lining cells of the alveoli are mainly formed of type II pneumocytes (▲). Some areas reveal cell laceration (\*). Mic. Mag. X 1500.

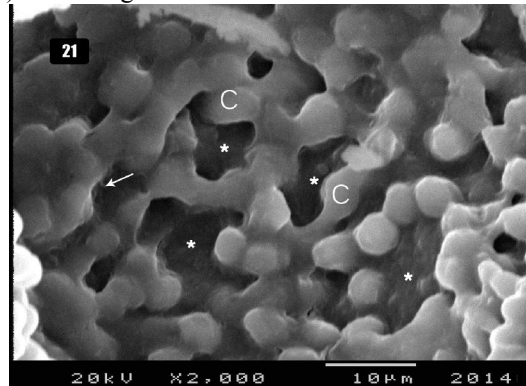


**Fig. 21:** A scanning electron photomicrograph of a section in the rat lung of group II showing the apical surface of the Clara cells (C) in the luminal surface of a bronchiole with loss of cilia in between them (\*). Some areas showed disorganization and atrophy of cilia (↑). Mic. Mag. X 2000.

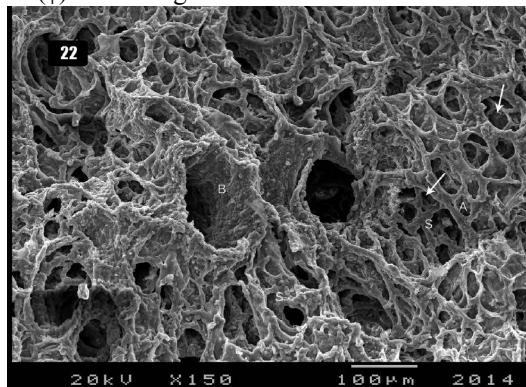


**Fig. 22:** A scanning electron photomicrograph of a section in the rat lung of group III showing apparent normal thickness of the smooth muscle layer (\*) of the bronchiole (B) and normal sized alveoli (A) which open in the air spaces by apparently normal sized opening (↑). Apparently normal sized inter-alveolar septa were observed (S). Mic. Mag. X 150.

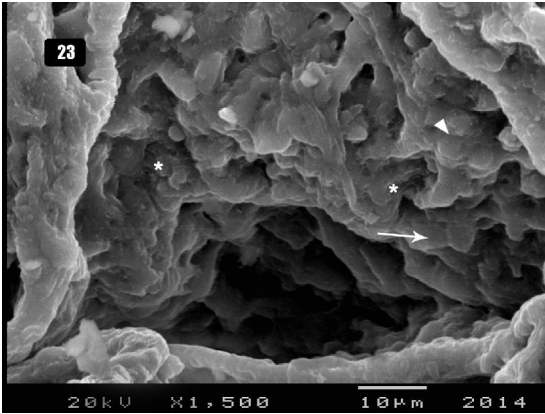


**Fig. 23:** A scanning electron photomicrograph of a section in the rat lung of group III showing that the lining cells of the alveoli are formed of type I pneumocytes ( $\uparrow$ ) and type II pneumocytes ( $\blacktriangle$ ). Few areas of the lining epithelium reveal damage of their cells (\*). Mic. Mag. X 1500.

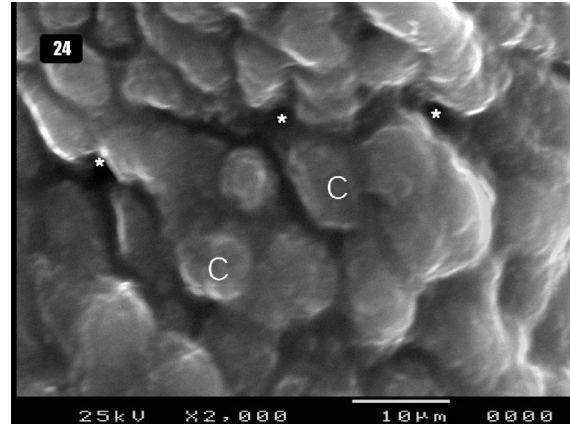


**Fig. 24:** A scanning electron photomicrograph of a section in the rat lung of group III showing the apical surface of the lining Clara cells (C) in the luminal surface of the bronchiole with loss of cilia in between them (\*). Mic. Mag. X 2000.

**Table 1: Means  $\pm$  SD of collagen fiber area %, alveolar wall area % and PCNA LI in different groups with their  $p$  values.**

Group	Collagen fiber area %	Alveolar wall area %	PCNA LI %
Group I	7.222 $\pm$ 1.288	49.209 $\pm$ 14.6272	5.48725 $\pm$ 1.12105
Group II	14.539 $\pm$ 4.133 $P < 0.001^*$ $P < 0.001^\#$	59.958 $\pm$ 6.9734 $P = 0.032^*$ $P = 0.001^\#$	17.31250 $\pm$ 1.74810 $P < 0.001^*$ $P < 0.001^\#$
Group III	6.821 $\pm$ 1.652 $P = 0.476^*$	43.264 $\pm$ 9.232 $P = 0.225^*$	9.77435 $\pm$ 2.28900 $P < 0.001^*$

SD = standard deviations. PCNA LI= PCNA Labeled Index.  $p$  value  $< 0.05$  is significant.  $p$  value  $< 0.01$  is highly significant. \*  $p$  value compared with group I. #  $p$  value compared with group III.

#### 4. Discussion

The potent and efficacious anti-dysrhythmic agent amiodarone can cause potentially life-threatening lung damage (amiodarone-induced pulmonary toxicity) which is characterized by cell death in the lungs, followed by inflammation and fibrosis. Amiodarone's major metabolite, desethylamiodarone, has a greater toxic potency than amiodarone and it has been suggested that desethylamiodarone may act synergistically with amiodarone to cause lung toxicity (Roth *et al.*, 2013).

In the current study, amiodarone administration to rats of group II led to thickening of the wall of pulmonary arterioles which can lead to the development of pulmonary hypertension (Sood *et al.*, 2011). Also, thick bronchiolar wall with obstruction of some bronchioles was seen. Thickened inter-alveolar septa, collapsed alveoli and intra-alveolar cellular debris were found. These findings were in

agreement with Zaglool *et al.* (2011) who investigated the effect of stem cell therapy on the amiodarone induced interstitial lung fibrosis in albino rat.

Intra-alveolar hemorrhage and presence of hyaline material as well as a lot of fibroblasts and macrophages in the alveolar lumen were detected in group II rats of the present work. These results were in line with Nacca *et al.* (2012) who added that the pathologic manifestations of patchy bronchiolitis obliterans, organizing pneumonia or diffuse alveolar damage were observed. They mentioned that the classic finding was the lipid-laden macrophages in alveolar spaces known as foam cells. Amiodarone has potent inhibitory effects on lysosomal phospholipase leading to accumulation of phospholipid bound drug in membrane-rich structures (Halliwell, 1997).

In this study, the alveolar wall of the group II rats showed mononuclear cell infiltration with extensive increase in collagen deposition. The lining epithelium of the alveoli was mainly formed of type II pneumocytes with areas revealing cell laceration. *Larsen et al. (2012)* found that these manifestations were due to a nonspecific interstitial pneumonitis predominantly composed of mononuclear cells, foamy alveolar macrophages, type II cell hyperplasia, and fibrosis. *Kapatou et al. (2010)* stated that the lung of amiodarone group revealed lack of lining alveolar epithelium. They were postulated that amiodarone induce apoptosis of alveolar epithelial cells in daily and cumulative dosages due to decreased intracellular anti-apoptotic proteins.

In the group II rats of the current study, the bronchiole's luminal surface exhibited loss of cilia in between the Clara cells in addition to disorganization and atrophy of cilia in some areas. Three different and intertwined mechanisms of lung toxicity have been suggested: (i) a direct toxic effect; (ii) an immune-mediated mechanism; and (iii) the angiotensin enzyme system activation (*Papiris et al., 2010*).

Significant increase in the area percentage of the inter-alveolar collagen fibers and alveolar wall area fraction were recorded in the group II rats of this study. *King et al. (2001)* demonstrated that the critical pathway to end-stage fibrosis is not in fact "alveolitis" but rather the ongoing epithelial damage and repair process associated with persistent fibroblastic proliferation. Correspondingly, it was documented that the histopathologic appearance of amiodarone pneumonitis included septal thickening, interstitial oedema, non-specific inflammation and fibrosis (*Schwaiblmair et al., 2010*). Amiodarone was found to upregulate angiotensinogen messenger RNA and angiotensin II was shown to promote fibrosis through stimulation of transforming growth factor (TGF)-beta1 (*Papiris et al., 2010*).

In the present study, significant increase in the PCNA labeling index (percent of nuclei immunostained for PCNA) of the alveolar cells of group II rats was noted. PCNA is a highly conserved cellular protein that functions both in DNA replication and in DNA repair (*Xu and Morris, 1999*). Deregulated inflammation and cellular damage are postulated to be important initiators of cell proliferation and fibrogenesis (*Thannickal et al., 2004*).

In the current study, the effect of selenium and combination of vitamins was investigated on the amiodarone-induced alveolar damage and fibrosis. Normal pulmonary arteriole, bronchioles and normal alveoli with thin inter-alveolar septa were seen in lung sections of group III rats. There was not any

detectable intra-alveolar hemorrhage, hyaline material or cellular debris. These results were in accordance with that of *Zidan (2011)* who used vitamin E as a protective from amiodarone induced lung damage. The previous author found that mild inter-alveolar septa thickening with mild inflammatory cellular infiltration was still obvious. Addition of selenium, vitamins C and A in this study may be factor for improving these findings. These findings were also in agreement with *Atli et al. (2012)* who proved prevention of lung damage due to sepsis after pretreatment with selenium and vitamin E in rat model.

The demonstrated damage of the alveolar and bronchiolar lining epithelium of group III rats was obviously lesser than that shown in group II rats. Also, the alveolar wall area percentages of group III rats exhibited insignificant differences as compared to that of the control group. *Hawker et al. (1993)* found an increase in glutathione peroxidase levels in blood and tissue (heart, liver, lung and spleen) of rats given selenium. Consistently, a protective role of vitamin E against oxidative stress injury and alteration in the architecture of liver and lungs of rats that received amiodarone was proved by *Zaki and Eid (2009)*. Also, *Cekic et al. (2011)* suggested that treatment with vitamin C might prevent amiodarone-induced toxicity in rat by restoring cellular glutathione content. Moreover, *Durukan et al. (2012)* documented the cytoprotective role of vitamin C in amiodarone induced cytotoxicity on cell culture media.

The inter-alveolar collagen fiber area percentages of group III rats in this study were within the normal values with highly significant decrease as compared to that of group II. This result was in accordance with *Card et al. (2003)* who proved a protective role for vitamin E in an in vivo model of amiodarone induced pulmonary toxicity, and suggested that this antioxidant might have non-specific antifibrotic effects in the lung.

As regards the PCNA labeled index of the alveolar parenchyma of group III rats, highly significant decrease was recorded in comparison with that of group II. Meanwhile, highly significant increase was documented as compared to that of the control rats. This finding could be due to cellular regeneration in the injured alveolar parenchyma (*Xu and Morris, 1999*).

#### **Conclusion:**

This study concluded that concomitant administration of selenium and combination of vitamins (vitamins A, E & C) has important preventive effects on the amiodarone-induced alveolar damage and fibrosis.

**Corresponding author**

Amal Abd El-khalek Mahdy,  
Anatomy and Embryology Department, Faculty of  
Medicine, Tanta University, Gharbia, Egypt.  
[mora2004@live.com](mailto:mora2004@live.com)

**References**

1. **Atli, M., Erikoglu, M., Kaynak, A., et al. 2012.** The effects of selenium and vitamin E on lung tissue in rats with sepsis. *Clin Invest Med* 35(2):E48-54.
2. **Bancroft, J.D. and Gamble, M. 2008.** Theory and practice of histological techniques. 6<sup>th</sup> ed., Churchill Livingstone, Edinburgh, London, England, 150.
3. **Bolt, M.W., Racz, W.J., Brien, J.F. and Massey, T.E. 2001.** Effects of vitamin E on cytotoxicity of amiodarone and N-desethylamiodarone in isolated hamster lung cells. *Toxicol*;166:109–18.
4. **Bozzola, J.J. and Russel, L.D. 1999.** Electron microscopy: Principles and Techniques for Biologists. 2<sup>nd</sup> ed. Boston, Jones and Baretlett, London, 48-202.
5. **Card, J.W., Racz, W.J., Brien, J.F. and Massey, T.E. 2003.** Attenuation of amiodarone-induced pulmonary fibrosis by vitamin E is associated with suppression of transforming growth factor-beta1 gene expression but not prevention of mitochondrial dysfunction. *J Pharmacol Exp Ther*; 304(1):277-283.
6. **Cekic, S. Pavlovic, D., Sarac, M. et al., 2011.** The effect of vitamin C on amiodarone-induced toxicity in rat thymocytes. *Cen Eur J Med*; 6(1):58-63.
7. **Chen, H. and Tappel, A.L. 1995.** Protection of vitamin E, selenium, trolox C, ascorbic acid palmitate, acetylcysteine, coenzyme Q0, coenzyme Q10, beta-carotene, canthaxanthin, and (+)-catechin against oxidative damage to rat blood and tissues in vivo. *Free Radic Biol Med*; 18(5):949-53.
8. **Coker, R.K. and Laurent, G.J. 1997.** Anticytokine approaches in pulmonary fibrosis: bringing factors into focus. *Thorax*; 52:294–6.
9. **Dawson-Saunders, B. and Trapp, R. 2001.** Basic and Clinical Biostatistics. 3<sup>rd</sup> ed. Lange Medical Books/McGraw-Hill, New York, 161-218.
10. **Durukan, A.B., Erdem, B., Durukan, E., et al., 2012.** May toxicity of amiodarone be prevented by antioxidants? A cell-culture study. *J Cardiothorac Surg*; 7(1):61.
11. **Foley, J.F. Dietrich, D.R., Swenberg, J.A. and Maronpot, R.R. 1991.** Detection and Evaluation of Proliferating Cell Nuclear Antigen (PCNA) in Rat Tissue by an Improved Immunohistochemical Procedure, *J Histotech*; 14(4):237-241.
12. **Halliwel, W.H. 1997.** Cationic amphiphilic drug-induced phospholipidosis. *Toxicol Pathol*; 25:53-60.
13. **Hawker, F.H., Ward, H.E., Stewart, P.M., et al., 1993.** Selenium deficiency augments the pulmonary toxic effects of oxygen exposure in the rat. *Eur Respir J*; 6(9):1317-23.
14. **Hemmati, A.A., Aghel, N., Nazari, Z., et al., 2006.** Grape seed extract can reduce the fibrogenic effect of bleomycin in rat lung. *Iranian J Pharm Sci*; 2:142.
15. **Izbicki, G., Segel, M.J., Christensen, T.G., et al., 2002.** Time course of bleomycin-induced lung fibrosis. *Int J Exp Pathol*; 83(3):111–119.
16. **Kapatou, E., Skyrlas, A., Agelaki, M.G., et al., 2010.** Amiodarone attenuates apoptosis, but induces phospholipidosis in rat alveolar epithelial cells. *J Physiol Pharmacol*; 61:671–677.
17. **King, T.E.Jr., Schwarz, M.I., Brown, K., et al., 2001.** Idiopathic pulmonary fibrosis: Relationship between histopathologic features and mortality. *Am J Respir Crit Care Med*; 164: 1025–1032.
18. **Kolettis, T.M., Agelaki, M.G., Baltogiannis, G.G., et al., 2007.** Comparative effects of acute vs. chronic oral amiodarone treatment during acute myocardial infarction in rats. *Europace*; 9:1099–1104.
19. **Konopacka, M. and Rzeszowska-Wolny, J. 2001.** Antioxidant vitamins C, E and  $\beta$ -caroten reduce DNA damage before as well as after  $\gamma$  irradiation of human lymphocytes in vitro. *Mutat Res*; 491(1-2):1-7.
20. **Korkolopoulou, P., Oates, J., Crocker, J. and Edwards, C. 1993.** p53 expression in oat and non-oat small cell lung carcinomas: correlations with proliferating cell nuclear antigen *J Clin Pathol*; 46(12):1093-1096.
21. **Larsen, B.T., Vaszar, L.T., Colby, T.V., and Tazelaar, H.D. 2012.** Lymphoid hyperplasia and eosinophilic pneumonia as histologic manifestations of amiodarone-induced lung toxicity. *Am J Surg Pathol*; 36(4):509-16.
22. **Nacca, N., Bhamidipati, C.M., Yuhico, L.S., et al., 2012.** Severe amiodarone induced pulmonary toxicity. *J Thorac Dis*; 4(6):667–670.
23. **Naidich, D.P., Srichai, M.B. and Krinsky, G.A. 2007.** Computed tomography and magnetic resonance of the thorax. Lippincott Williams & Wilkins, Philadelphia.

24. **O'Brien, K., Troendle, J., Gochuico, B.R., et al., 2011.** Pirfenidone for the treatment of Hermansky-Pudlak syndrome pulmonary fibrosis. *Mol Genet Metab*; 103:128–134.
25. **Papiris S.A., Triantafillidou, C., Kolilekas, L., et al., 2010.** Amiodarone: review of pulmonary effects and toxicity. *Drug Saf*; 33:539–558.
26. **Punithavathi, D., Venkatesan, N. and Babu, M. 2003.** Protective effects of curcumin against amiodarone-induced pulmonary fibrosis in rats. *Br J Pharmacol*; 139:1342–50.
27. **Refaat, S.H. 2007.** The protective role of antioxidants against gamma irradiation-induced injury of the liver and lung in male albino rats. *Egypt J Anat*; 30(1&2): 69-90.
28. **Roth, F.C., Mulder, J.E., Brien, J.F., et al., 2013.** Cytotoxic interaction between amiodarone and desethylamiodarone in human peripheral lung epithelial cells. *Chem Biol Interact*; 204(3):135-9.
29. **Schwaiblmair, M., Berghaus, T., Haeckel, T., et al., 2010.** Amiodarone-induced pulmonary toxicity: an under- recognized and severe adverse effect? *Clin Res Cardiol: official journal of the German Cardiac Society*; 99:693–700.
30. **Sood, B.G., Wykes, S., Landa, M., et al., 2011.** Expression of eNOS in the lungs of neonates with pulmonary hypertension. *Exp Mol Pathol*; 90:9–12.
31. **Thannickal, V.J., Toews, G.B., White, E.S., et al., 2004.** Mechanisms of pulmonary fibrosis. *Annu Rev Med*; 55:395–417.
32. **Xu, J. and Morris, G.F. 1999.** p53-Mediated Regulation of Proliferating Cell Nuclear Antigen Expression in Cells Exposed to Ionizing Radiation. *Mol Cell Biol*; 19(1) 12-20.
33. **Zaglool, S.S., Zickri, M.B.A, Abd El Aziz, D.H., et al., 2011.** Effect of Stem Cell Therapy on Amiodarone Induced Fibrosing Interstitial Lung Disease in Albino Rat. *Int J Stem Cells*; 4(2): 133–142.
34. **Zaki, M.S.and Eid, R.A. 2009.** Role of vitamin-E on rat liver-amiodarone: an ultrastructural study. *Saudi J Gastroenterol*; 15(2):104-110.
35. **Zhang, K. and Phan, S.H. 1996.** Cytokines and pulmonary fibrosis. *Biol Signals*; 5:232–9.
36. **Zidan, R.A. 2011.** Effect of long-term administration of amiodarone on rat lung and the possible protective role of vitamin E: a histological and immunohistochemical study. *Egypt J Histol*; 34:117-128.

4/22/2014